Available online at www.sciencedirect.com
ScienceDirect
Journal of Power Sources 169 (2007) 355–360
JOURNAL OF POWER SOURCES
www.elsevier.com/locate/jpowsour

Short communication

Electrochemical intercalation of lithium in the titanium hydrogeno phosphate $Ti(HPO_4)_2 \cdot H_2O$

M. Satya Kishore [a,*], V. Pralong [a], V. Caignaert [a], U.V. Varadaraju [b], B. Raveau [a]

[a] *Laboratoire CRISMAT, UMR 6508 CNRS ENSICAEN, 6 bd Maréchal Juin, 14050 CAEN Cedex, France*
[b] *Materials Science Research Centre, Indian Institute of Technology Madras, Chennai 600036, India*

Received 4 September 2006; received in revised form 13 March 2007; accepted 16 March 2007
Available online 30 March 2007

Abstract

The electrochemical reactivity of the layered titanium hydrogeno phosphate $Ti(HPO_4)_2 \cdot H_2O$ versus lithium has been studied. Lithium intercalation occurs at ~2.5 V with low polarization, leading to a new lithiated Ti(III) phase, $LiTi(HPO_4)_2 \cdot H_2O$. $Ti(HPO_4)_2 \cdot H_2O$ exhibits a reversible capacity of 80 mAh g^{-1} in the voltage window 1.8–3.5 V at *C*/10 rate. The stable reversible capacity reveals that the presence of H_2O lattice is not affecting the electrochemical reaction. The reversibility of the reaction is demonstrated by extracting lithium from $LiTi(HPO_4)_2 \cdot H_2O$ and the host structure is intact. The electrochemical behaviour of dehydrated phases $Ti(HPO_4)_2$ and TiP_2O_7 has also been investigated.

Keywords: Li-ion battery; $Ti(HPO_4)_2 \cdot H_2O$; Lithium intercalation

1. Introduction

Phosphates with a three-dimensional structure containing transition metals such as Fe, Ti, or V are of recent interest in view of their potential application as electrode materials in secondary lithium ion batteries. In particular, Ti based materials with Ti^{4+}/Ti^{3+} redox couple have been studied as cathode materials. In the early 1970s, TiS_2 has been used as a cathode material in commercial rechargeable lithium batteries, which operate at 2.1 V [1]. Later, good reversibility of Ti^{4+}/Ti^{3+} redox couple was found in oxides such as $Li_4Ti_5O_{12}$ with spinel structure [2–4], in nanowires of TiO_2 [5] and in the ternary oxide, $Li_2SrTi_6O_{14}$, with 3D structure [6]. However, the redox potential is low (~1.5 V) in these oxides. Thus, it has been proposed that $Li_4Ti_5O_{12}$ can be used as an anode material by combining it with high voltage cathode materials such as $LiMn_{2-x}M_xO_4$ [7,8]. On the other hand, in phosphates with the nasicon structure, $LiTi_2(PO_4)_3$ exhibits lithium intercalation/deintercalation process at ~2.5 V reversibly [9]. Patoux and Masquelier have studied lithium insertion in different titanium based hosts such as phosphates, silicates, sulfates and analyzed the inductive effect of polyhedral groups on the redox potential of Ti^{4+}/Ti^{3+} [10].

Recently, electrochemical intercalation of Li into several phosphates containing lattice water such as $FePO_4 \cdot 2H_2O$ [11], $Fe_{1.18}PO_4(OH)_{0.57}(H_2O)_{0.43}$ [12], $Fe_{1.19}PO_4F_{0.11}(OH)_{0.46}(H_2O)_{0.43}$ [13], $Fe_4(P_2O_7)_3 \cdot nH_2O$ [14], $(H_3O)[Fe(H_2O)][H_8(PO_4)_6] \cdot 3H_2O$ [15], $VOPO_4 \cdot 2H_2O$ [16] has been reported. It has been observed that the presence of H_2O does not affect the electrochemical performance. Thus, we begin exploring hydrated titanium phosphates as lithium intercalation hosts. In the system H–Ti–P–O, numerous titanium hydrogeno phosphates are known with different structures. α-$Ti(HPO_4)_2 \cdot H_2O$ has a lamellar structure with large interlayer spacing [17–19]. The compound is isostructural with α-$Zr(HPO_4)_2 \cdot H_2O$, which is made up of layers formed by $PO_3(OH)$ tetrahedra and TiO_6 octahedra. The molecules of water of crystallization are located in between the layers and participate in the hydrogen-bond network with acidic protons present on the phosphate groups. The neighbouring layers are held together by van der Waals forces. The acidic proton can be ion exchanged easily with mono or divalent cations such as Li^+, Na^+, K^+, Ca^{2+}, Pd^{2+} and hence the compound is considered to

* Corresponding author. Tel.: +33 2 31 45 26 32; fax: +33 2 31 95 16 00.
E-mail address: kishore@ensicaen.fr (M.S. Kishore).

0378-7753/$ – see front matter © 2007 Elsevier B.V. All rights reserved.
doi:10.1016/j.jpowsour.2007.03.051

be a good cation exchanger [20–23]. In addition, the structure is amenable to intercalation of organic molecules such as alkyl diamines [24,25]. Although, several intercalation reactions of $Ti(HPO_4)_2{\cdot}H_2O$ have been reported, to the best of our knowledge, the possible intercalation of Li into this compound has not been studied. In the present work, we report the intercalation of lithium electrochemically into $Ti(HPO_4)_2{\cdot}H_2O$. We demonstrate the reversible intercalation/deintercalation of lithium in this phase, leading to a new hydrated Ti(III) phase, $LiTi(HPO_4)_2{\cdot}H_2O$.

2. Experimental

2.1. Synthesis

The synthesis of $Ti(HPO_4)_2{\cdot}H_2O$ was carried out by dissolving titanium metal in phosphoric acid [26]. Typically, 0.5 g of titanium metal (Merck, 99%) was stirred in 20 ml of H_3PO_4 (Aros organics, 85% solution in water) at 170 °C until the metal dissolved completely and the solution turned blue, which is an indication of Ti being present in +3 oxidation state. The solution was kept at this temperature for 24 h followed by cooling to RT leading to the formation of a white precipitate. The precipitate was washed with water and dried at 60 °C.

The dehydrated phases $Ti(HPO_4)_2$, TiP_2O_7 were obtained by heating $Ti(HPO_4)_2{\cdot}H_2O$ for 12 h at 280 and 800 °C, respectively.

2.2. Physical characterizations

The powder X-ray diffraction pattern was registered in the 2θ range of 5–100° using a Philips X'pert diffractometer with Bragg-Brentano geometry (Cu Kα radiation; $\lambda_{Cu\ K\alpha} = 1.5406$ Å). A scanning electron microscope (SEM) (Philips Field Effect Gun (FEG) XL-30) was used to study the morphology. Thermogravimetric studies were carried out with a Setaram TG 92 instrument at a heating rate of 2 °C min^{-1} under flowing nitrogen gas.

The titanium hydrogeno phosphate samples were tested as positive electrode materials in Swagelok type cells. The cells were assembled in an argon filled glove box, with lithium metal as the negative electrode and a borosilicate glass fiber sheet as a separator with a saturated amount of 1 M $LiPF_6$ in 1:1 ethylene carbonate (EC):dimethyl carbonate (DMC) (LP30, Merck) as the electrolyte. The composite positive electrode was prepared by mixing 70 wt.% active material with 20 wt.% acetylene black and 10 wt.% PVDF in 1-methyl-2-pyrrolidinone (NMP). The electrochemical reactivity was monitored with a VMP II potentiostat/galvanostat (Biologic SA, Claix, France) at room temperature (25 °C). Electrochemical cycling was performed at different voltage windows, viz., 1.8–3.5, 1.7–3.5, 1.5–3.5 V at *C*/10 rate for $Ti(HPO_4)_2{\cdot}H_2O$, $Ti(HPO_4)_2$ and TiP_2O_7, respectively. Potentiostatic intermittent titration technique (PITT) experiment was performed on $Ti(HPO_4)_2{\cdot}H_2O$ in the voltage window 1.8–3.5 V in steps of 10 mV, wherein after each 1 h interval the voltage is increased to the next step. For galvanostatic intermittent titration technique (GITT) on $Ti(HPO_4)_2$, constant current flux (0.1 mA, *C*/10) is applied for 1 h and the cell is maintained at zero current for 1 h. This procedure is repeated in the voltage window 1.7–3.3 V.

3. Results and discussion

3.1. Phase characterization

XRD patterns of $Ti(HPO_4)_2{\cdot}H_2O$, $Ti(HPO_4)_2$ and TiP_2O_7 with SEM pictures (inset) are given in Fig. 1. The XRD pattern of

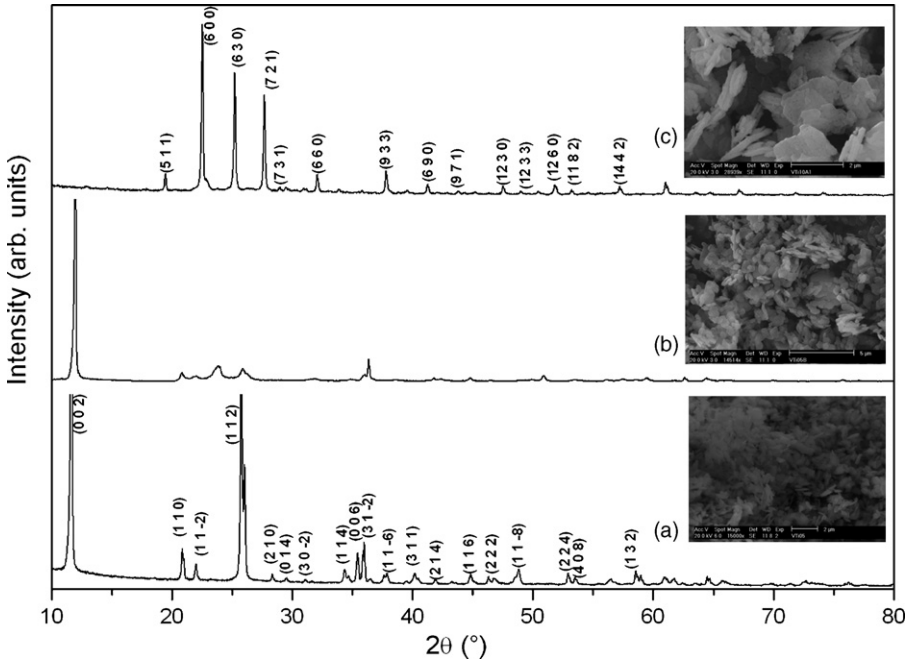

Fig. 1. Powder XRD patterns of (a) $Ti(HPO_4)_2{\cdot}H_2O$, (b) $Ti(HPO_4)_2$ and (c) TiP_2O_7. SEM picture of the corresponding phase is given in the inset.

$Ti(HPO_4)_2{\cdot}H_2O$ (Fig. 1a) is indexed on the basis of monoclinic cell with space group $P2_1/n$. The presence of sharp peaks reveals the formation of a well crystalline phase and the refined lattice parameters are $a = 8.6337$ (1) Å, $b = 5.0052$ (3) Å, $c = 15.5035$ (3) Å; $\beta = 101.322$ (1)°, which are in good agreement with previous reports [19]. From the SEM picture (Fig. 1a, inset), it can be seen that the particles are homogeneous in shape and size with an average particle size of about 0.5 μm. It is known that, in acidic titanium phosphates, the water content varies with the synthesis method and temperature. In order to estimate the number of moles of H_2O present in the lattice, we have characterized the sample by TGA. The TGA curve presents two steps (Fig. 2a). The first step with onset above 100 °C can be attributed to the loss of one water molecule, whereas the second step with onset above 400 °C corresponds to the dehydroxylation, leading to the formation of pyrophosphate. The total weight loss is about 15%, indicating the loss of ~2 moles of water per mole of compound. Fig. 2b shows the *in situ* XRD patterns of $Ti(HPO_4)_2{\cdot}H_2O$ recorded as a function of temperature. It is evident from the XRD patterns that a new peak is observed at higher 2θ while the peak corresponding to (0 0 2) disappears. This is due to the formation of the dehydrated phase and at 280 °C the hydrated phase disappears completely, indicating the formation of pure $Ti(HPO_4)_2$. On heating above 280 °C, a new peak is observed at $2\theta = 12.3°$, which is due to the formation of layered pyrophosphate [27].

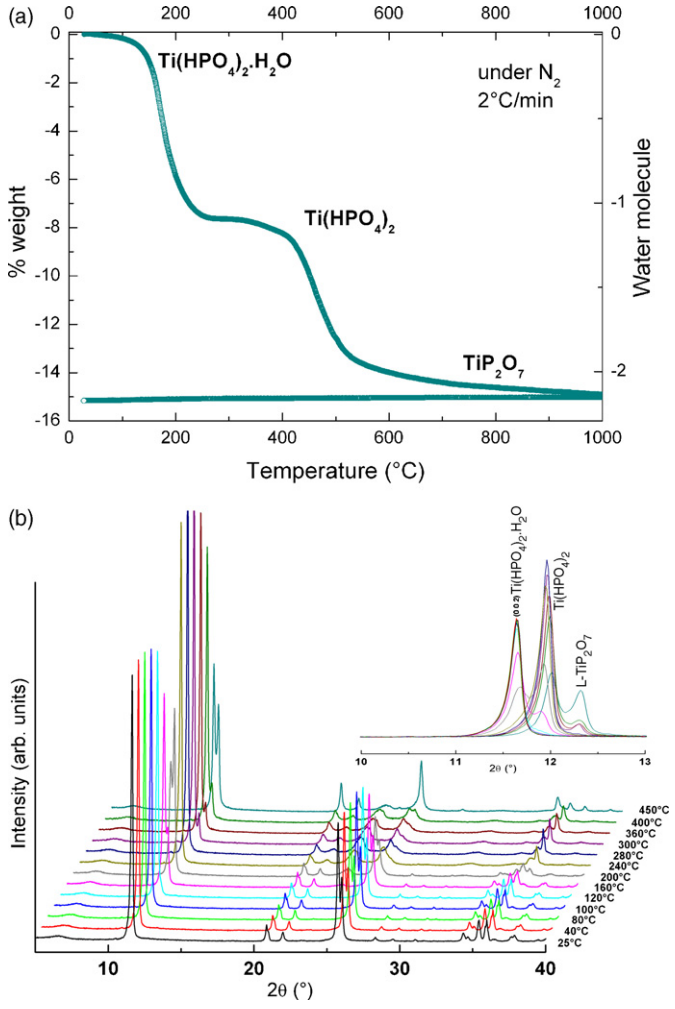

Fig. 2. (a) TGA curve of $Ti(HPO_4)_2{\cdot}H_2O$ under N_2 gas at 2 °C min^{-1}. (b) XRD patterns of $Ti(HPO_4)_2{\cdot}H_2O$ as a function of temperature performed in heat chamber under N_2.

The XRD pattern of $Ti(HPO_4)_2$ is given in Fig. 1b. Due to the presence of only a few reflections and since no structural data is available in the literature on this phase, it is difficult to index the pattern and refine the structure. However, the XRD pattern is similar to the one reported by Dzyuba et al. [17] confirming the formation of the phase. The particle size and morphology are similar to that of $Ti(HPO_4)_2{\cdot}H_2O$. The XRD pattern of the pyrophosphate, TiP_2O_7, formed by heating the parent phase at 800 °C is given in Fig. 1c. The compound crystallizes in cubic system (ICSD No. 038-1468) and SEM picture indicates agglomeration of the particles with an average size of 1–2 μm.

3.2. Electrochemical characterization

The discharge and charge curves of $Ti(HPO_4)_2{\cdot}H_2O$ are shown in Fig. 3a. During the initial discharge, 1Li is intercalated and further cycling was carried out in the voltage window 1.8–3.5 V at $C/10$ rate. A plateau at ~2.5 V is observed with an initial discharge capacity of 103 mAh g^{-1}. The voltage is characteristic of Ti^{4+}/Ti^{3+} redox couple as observed in other Ti phosphates [10,28]. During the first charge, 87 mAh g^{-1} is observed at ~2.7 V. Although there is an irreversible capacity loss of about 20% during the first cycle, on subsequent cycling the capacity is stable. The plot of dx/dV versus voltage indicates sharp reduction and oxidation peaks at 2.53 and 2.64 V, respectively (Fig. 3a, inset). The sharp peaks in the differential plot suggest the co-existence of two phases. This can be further seen by PITT (Fig. 3b). PITT reveals a bell shaped response of the current characteristic of a two-phase reaction [29,30]. Further, decrease in discharge capacity is observed when the C-rate is increased from $C/10$ to $1C$, indicating that kinetics of intercalation of Li^+ is slow. At the end of 50 cycles, a reversible capacity of 80 mAh g^{-1} (~0.8Li) is observed (Fig. 4) at $C/10$ rate. This demonstrates the stability of the layered phosphate structure towards reversible lithium intercalation.

To examine the structural changes accompanying lithium intercalation/deintercalation in $Ti(HPO_4)_2{\cdot}H_2O$, *ex situ* XRD patterns were recorded on phases corresponding to intercalation of 0.5 and 1Li and after charge to 3.5 V corresponding to a phase with composition $Li_{0.2}Ti(HPO_4)_2{\cdot}H_2O$. The XRD patterns are shown in Fig. 5. The lithiated phase is found to be stable in air for a few days and the long-term stability under moisture/air has not been checked. The XRD patterns show that the structural integrity is maintained with lithium intercalation/deintercalation indicating that the layer structure is retained with lithium intercalation and also suggesting that the electrochemical cycling has no influence on H_2O content. A slight shift in the high intense (0 0 2) peak is observed upon lithium intercalation. Intercalation of 1Li leads to the splitting of the peaks at higher 2θ (25.97°), which is clearly seen in the inset of Fig. 5. The volume of the cell increases slightly from 656.98 to 673.81 Å^3 and the lithiated

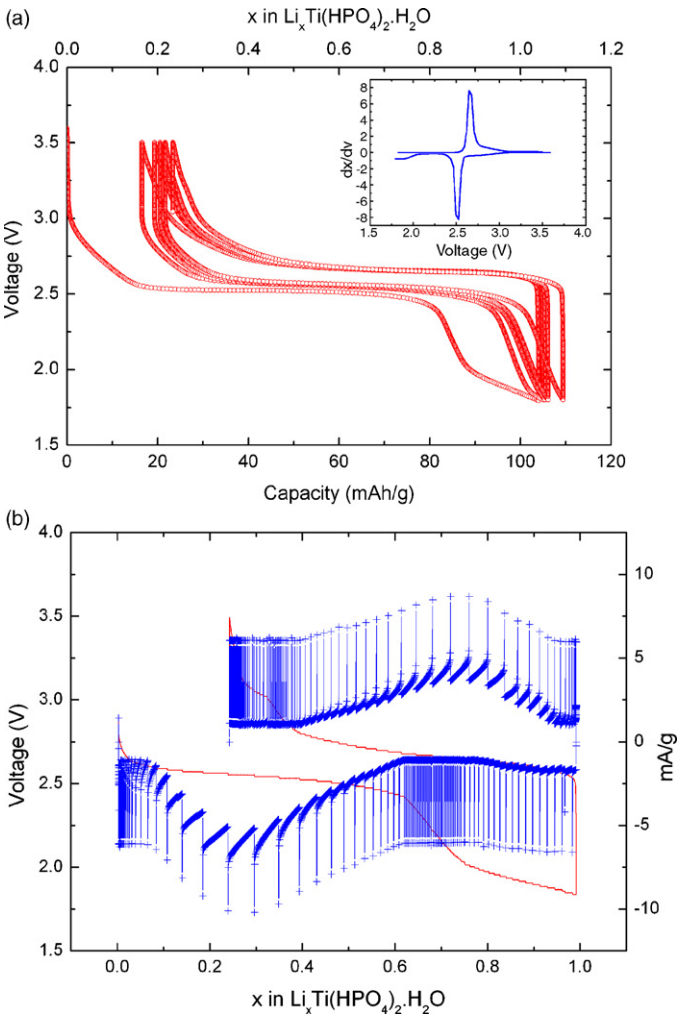

Fig. 3. (a) Discharge–charge curves of $Ti(HPO_4)_2{\cdot}H_2O$ vs. Li^+/Li at *C*/10 rate. (b) Potentiometric titration curve (PITT) obtained for $Li/Ti(HPO_4)_2{\cdot}H_2O$ cell at a scan rate of 10 mV h^{-1}.

phase can be indexed on a triclinic cell. The distortion could be a result of intercalation of Li^+ while reduction of Ti^{4+} to Ti^{3+}. Thus, we have synthesized electrochemically a new lithiated phase containing Ti^{3+}, $LiTi(HPO_4)_2{\cdot}H_2O$. However, we are

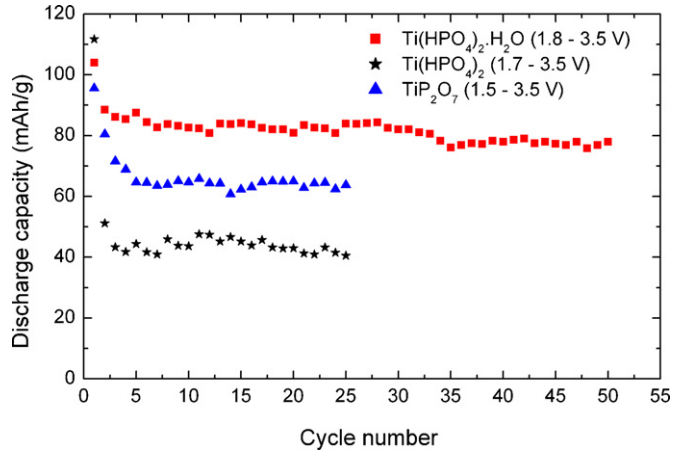

Fig. 4. Cycling performance of $Ti(HPO_4)_2{\cdot}H_2O$, $Ti(HPO_4)_2$, and TiP_2O_7 at *C*/10 rate.

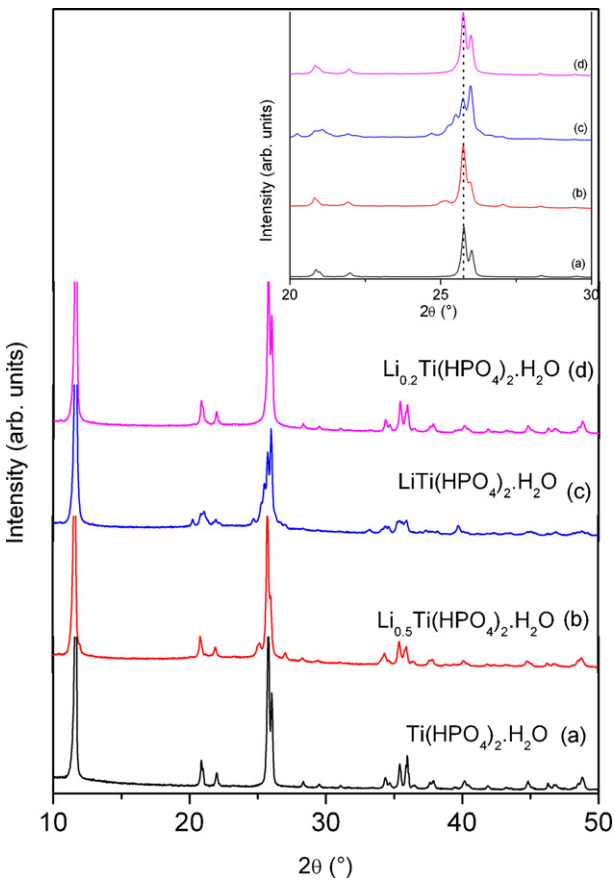

Fig. 5. Ex situ XRD patterns of $Ti(HPO_4)_2{\cdot}H_2O$ electrode taken during initial cycle: (a) pristine compound, (b) after 0.5 intercalation, (c) after 1Li intercalation and (d) after charge to 3.5 V.

unable to derive the structure of this new phase by using the powder X-ray data. Neutron diffraction studies will be necessary to solve the structure. The XRD pattern after initial charge to 3.5 V is shown in Fig. 5d. The peaks become sharp again and the positions match with those of the parent phase without the presence of second phase. This shows the parent structure is retained with good crystallinity upon lithium extraction. The origin of the good reversibility of lithium intercalation in $Ti(HPO_4)_2{\cdot}H_2O$ can be explained by the fact that lithium intercalation involves only minimal changes in the structure.

The electrochemical behaviour of the dehydrated phase, $Ti(HPO_4)_2$ is shown in Fig. 6. The charge–discharge profiles of the first five cycles carried out at *C*/10 rate (a) and the results of GITT measurements (b) are shown for comparison. The initial discharge capacity with a lower cut-off voltage of 1.7 V is 112 mAh g^{-1}. The initial discharge profile of $Ti(HPO_4)_2$ is qualitatively different from that of $Ti(HPO_4)_2{\cdot}H_2O$. A small plateau at 2.5 V is observed during initial discharge, corresponding to intercalation of 0.2Li followed by intercalation of Li at ~1.75 V. By discharging the cell at slow rate (*C*/100) the initial plateau at 2.5 V is extended up to intercalation of ~0.5Li (not shown in figure). The GITT study also shows that during relaxation the voltage increases to the 2.5 V plateau value, suggesting that there is a large polarization [31]. In addition, we have performed ex situ XRD experiments to identify the

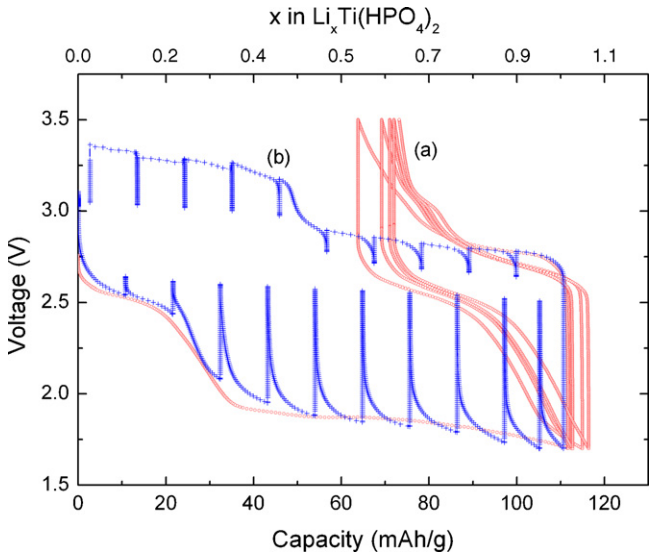

Fig. 6. (a) Voltage profiles of Li/Ti(HPO$_4$)$_2$ cell at *C*/10 rate. (b) Discharge and charge curves of Ti(HPO$_4$)$_2$ under GITT mode.

phase changes. The structural changes look complex and since the parent phase structure is not known it is difficult to draw any conclusions regarding structural changes. When the cell is cycled at *C*/10 rate, after the initial discharge, lithium intercalation/deintercalation is observed at ∼2.5 V with a low reversible capacity of 40 mAh g^{-1} (Fig. 4).

The charge–discharge curves of TiP_2O_7 are shown in Fig. 7. An initial discharge capacity of 90 mAh g^{-1} is observed with a lower discharge cut-off voltage of 1.5 V, corresponding to intercalation of 0.75Li. A plateau at ∼2.5 V is observed with a reversible capacity of ∼60 mAh g^{-1} (∼0.5Li) in the voltage range of 1.5–3.5 V (Fig. 4). The electrochemical behaviour of TiP_2O_7 was first reported by Uebou et al. [32], wherein 1Li is intercalated down to 1.0 V and their cycling behaviour was not studied. However, very recently, reversible capacity of ∼90 mAh g^{-1} was reported for mesoporous TiP_2O_7 in the voltage range of 1.5–4.0 V at *C*/10 rate [33] and about 100 mAh g^{-1} in the voltage window 2.0–3.4 V at *C*/10 rate for the sample synthesized by sol–gel method [10]. In both cases, the particle size is lower than that of the sample synthesized by us (1–2 μm). The large particle size increases the diffusion path length for Li^+ ion and could be the contributing factor for the observed low reversible capacity in the present study.

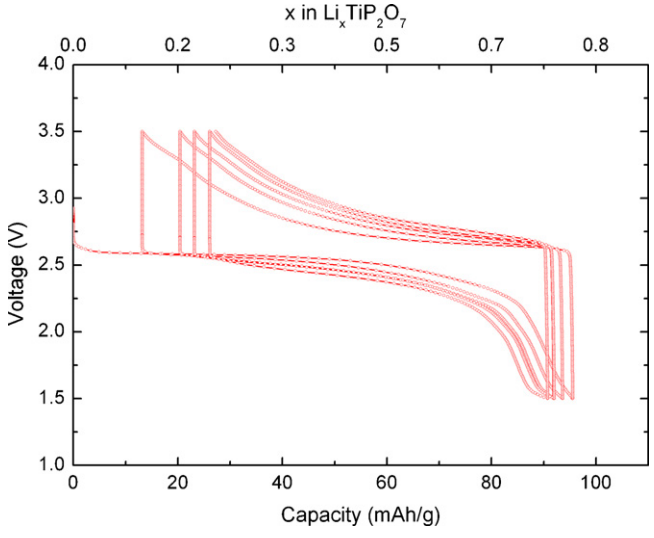

Fig. 7. Discharge–charge curves of Li/TiP_2O_7 cell in the voltage window 1.5–3.5 V at *C*/10 rate.

4. Conclusion

Reversible lithium intercalation/deintercalation is demonstrated in the titanium hydrogeno phosphate Ti(HPO$_4$)$_2$·H$_2$O. Lithium intercalation process occurs via a two-phase reaction at 2.5 V with a reversibility of ∼0.8Li. The structural stability upon lithium intercalation/deintercalation enables good reversibility in Ti(HPO$_4$)$_2$·H$_2$O. Although, it exhibits a flat voltage plateau at 2.5 V, the low reversible capacity (80 mAh g^{-1}) limits its application in Li-ion batteries. In addition, the study reveals the formation of a new lithiated Ti(III) phase LiTi(HPO$_4$)$_2$·H$_2$O, whose detailed structure and ionic conductivity will be reported in a forthcoming paper. The dehydrated products, viz., Ti(HPO$_4$)$_2$ and TiP_2O_7 have shown minimal electrochemical activity.

Acknowledgements

Financial support from IFCPAR (Indo-French Centre for the Promotion of Advanced Research/Centre Franco-Indien Pour la Promotion de la Recherche Avancee) and LAFICS program is gratefully acknowledged.

References

[1] M.S. Whittingham, Prog. Solid State Chem. 12 (1978) 41–99.
[2] T. Ohzuku, A. Ueda, N. Yamamoto, J. Electrochem. Soc. 142 (1995) 1431–1435.
[3] K. Nakahara, R. Nakajima, T. Matsushima, H. Majima, J. Power Sources 117 (2003) 131–136.
[4] L. Aldon, P. Kubaik, M. Womes, J.C. Jumas, J. Olivier-Fourcade, J.L. Tirado, J.I. Corredor, C.P. Vicente, Chem. Mater. 16 (2004) 5721–5725.
[5] P.G. Bruce, Solid State Sci. 7 (2005) 1456–1463.
[6] I. Belharouak, K. Amine, Electrochem. Commun. 5 (2003) 435–438.
[7] E. Ferg, R.J. Gummow, A. de Kock, M.M. Thackeray, J. Electrochem. Soc. 141 (1994) L147–L150.
[8] S. Panero, D. Satolli, M. Salomon, B. Scrosati, Electrochem. Commun. 2 (2000) 810–813.
[9] A. Nadiri, C. Delmas, C. R. Acad. Sci. Paris II 304 (1987) 415–417.
[10] S. Patoux, C. Masquelier, Chem. Mater. 14 (2002) 5057–5068.
[11] K. Zaghib, C.M. Julien, J. Power Sources 142 (2005) 279–284.
[12] Y. Song, P.Y. Zavalij, N.A. Chernova, M.S. Whittingham, Chem. Mater. 17 (2005) 1139–1147.
[13] M. Dollé, S. Patoux, T.J. Richardson, J. Power Sources 144 (2005) 208–213.
[14] C. Masquelier, P. Reale, C. Wurn, M. Morcrette, L. Dupont, D. Larcher, J. Electrochem. Soc. 149 (2002) A1037–A1044.
[15] V. Pralong, V. Caignaert, B. Raveau, Solid State Ionics 177 (2006) 2453–2456.
[16] N. Dupré, J. Gaubicher, T. Le Mercier, G. Wallez, J. Angenault, M. Quarton, Solid State Ionics 140 (2001) 209–221.
[17] E.D. Dzyuba, V.V. Pechkovskii, G.I. Salonets, L.S. Strugach, N.A. Ivkovich, Russ. J. Inorg. Chem. 21 (1976) 341–343.

[18] M.A. Salvadó, P. Pertierra, S. Garcia-Granda, J.R. Garcia, J. Rodriguez, M.T. Fernàndez-Diaz, Acta Crystallogr. B 52 (1996) 896–898.
[19] S. Bruque, M.A.G. Aranda, E.R. Losilla, P. Olivera-Pastor, P. Maireles-Torres, Inorg. Chem. 34 (1995) 893–899.
[20] R. Llavona, M. Suárez, J. Garcia, J. Rodriguez, Inorg. Chem. 28 (1989) 2863–2868.
[21] L.M. Nunes, C. Airoldi, Thermochim. Acta 328 (1999) 297–305.
[22] B.B. Sahu, K. Parida, J. Colloid Interf. Sci. 248 (2002) 221–230.
[23] C. Ferragina, P. Caferelli, P. Giannoccaro, Mater. Res. Bull. 33 (1998) 1635–1652.
[24] A. Espina, F. Menéndez, E. Jaimez, S.A. Khainakov, C. Trobajo, J.R. Garcia, J. Rodriguez, Mater. Res. Bull. 33 (1998) 763–771.
[25] A. Espina, E. Jaimez, S.A. Khainakov, C. Trobajo, J.R. Garcia, J. Rodriguez, Chem. Mater. 10 (1998) 2490–2496.
[26] P.-E. Tegehall, Acta Chem. Scand. A 40 (1986) 507–514.
[27] G. Ramis, G. Busca, V. Lorenzelli, A. La Ginestra, P. Galli, M.A. Massuccu, J. Chem. Soc., Dalton Trans. 4 (1988) 881–886.
[28] S. Patoux, G. Rousse, J.-B. Leriche, C. Masquelier, Solid State Sci. 6 (2004) 1113–1120.
[29] A. Martinez-de la cruz, F.E. Longoria Rodriguez, J.I. Rodiguez, Solid State Ionics 176 (2005) 2625–2630.
[30] S. Jouanneau, A. Verbaere, D. Guyomard, J. Solid State Chem. 172 (2003) 116–122.
[31] V. Legagneur, J.-H. Liao, Y. An, A. Le Gal La Salle, A. Verbaere, Y. Piffard, D. Guyomard, Solid State Ionics 133 (2000) 161.
[32] Y. Uebou, S. Okada, M. Egashira, J.-I. Yamaki, Solid State Ionics 148 (2002) 323–328.
[33] Z. Shi, Q. Wang, W. Ye, Y. Li, Y. Yang, Micropor. Mesopor. Mater. 88 (2006) 232–237.